Atmos. Chem. Phys. Discuss., 10, 18561–18605, 2010
www.atmos-chem-phys-discuss.net/10/18561/2010/
doi:10.5194/acpd-10-18561-2010

Atmospheric Chemistry and Physics Discussions

Evaluation of various observing systems for the global monitoring of CO_2 surface fluxes

K. Hungershoefer[1,*], F.-M. Breon[1], P. Peylin[1,2], F. Chevallier[1], P. Rayner[1,], A. Klonecki[3], and S. Houweling[4,5]**

[1]Laboratoire des Sciences du Climat et de l'Environnement (LSCE), Unité Mixte de Recherche, UMR1572, CNRS-CEA-UVSQ, 91191 Gif-sur-Yvette, France
[2]Laboratoire Biogéochimie et Ecologie des Milieux Continentaux, CNRS-UPMC-INRA, Paris, France
[3]Noveltis, 31520 Ramonville Saint Agne, France
[4]SRON Netherlands Institute for Space Research, Sorbonnelaan 2, 3584 CA Utrecht, The Netherlands
[5]Institute for Marine and Atmospheric Reasearch Utrecht, Princetonplein 5, 3584 CC Utrecht, The Netherlands
[*]now at: Deutscher Wetterdienst, Department Climate Monitoring, 63067 Offenbach, Germany
[**]now at: the University of Melbourne, School of Earth Sciences, Melbourne, Australia

Received: 13 July 2010 – Accepted: 17 July 2010 – Published: 5 August 2010

Correspondence to: K. Hungershoefer (katja.hungershoefer@lsce.ipsl.fr)

Published by Copernicus Publications on behalf of the European Geosciences Union.

ACPD
10, 18561–18605, 2010

Abstract

In the context of raising greenhouse gas concentrations, and the potential feedbacks between climate and the carbon cycle, there is an urgent need to monitor the exchanges of carbon between the atmosphere and both the ocean and the land surfaces. In the so-called top-down approach, the surface fluxes of CO_2 are inverted from the observed spatial and temporal concentration gradients. The concentrations of CO_2 are measured in-situ at a number of surface stations unevenly distributed over the Earth while several satellite missions may be used to provide a dense and better-distributed set of observations to complement this network. In this paper, we compare the ability of different CO_2 concentration observing systems to constrain surface fluxes. The various systems are based on realistic scenarios of sampling and precision for satellite and in-situ measurements.

It is shown that satellite measurements based on the differential absorption technique (such as those of SCIAMACHY, GOSAT or OCO) provide more information than the thermal infrared observations (such as those of AIRS or IASI). The OCO observations will provide significantly better information than those of GOSAT. A CO_2 monitoring mission based on an active (lidar) technique could potentially provide an even better constraint. This constraint can also be realized with the very dense surface network that could be built with the same funding as that of the active satellite mission. Despite the large uncertainty reductions on the surface fluxes that may be expected from these various observing systems, these reductions are still insufficient to reach the highly demanding requirements for the monitoring of anthropogenic emissions of CO_2 or the oceanic fluxes at a spatial scale smaller than that of oceanic basins. The scientific objective of these observing system should therefore focus on the fluxes linked to vegetation and land ecosystem dynamics.

ACPD

10, 18561–18605, 2010

1 Introduction

Carbon dioxide is a very important trace gas in the atmosphere and contributes significantly to the natural greenhouse effect, which enables life on Earth. Before the beginning of the industrialisation in the mid 18th century, the atmospheric carbon dioxide concentration was relatively constant for several thousand years with values between 250 and 290 ppm (IPCC, 2007). Since 1750, the anthropogenic CO_2 emissions from fossil fuel combustion, cement production, deforestation and land use changes (IPCC 2007) have led to an increase of the CO_2 concentration and a human-caused intensification of the greenhouse effect. Although more than half of the anthropogenic CO_2 emissions have been absorbed by natural carbon sinks on land and in the ocean, the atmospheric CO_2 concentration currently amounts to more than 386 ppm, i.e. 40% higher than the pre-industrial value. In addition, the fraction of CO_2 emissions that remains in the atmosphere has increased (Le Quéré et al., 2009). One reason for this is the rapid growth in fossil fuel emissions since 2000 due to the recent growth of the world economies. Another reason is a decline in the efficiency of the natural sinks in absorbing anthropogenic emissions (Canadell et al., 2007).

Our understanding of the sources and sinks is continuously improving. Estimates of the anthropogenic and contemporary air-sea CO_2 fluxes were recently published (Gruber et al., 2009). Model simulations suggest that the biosphere sink may decrease or even become a source (Cox et al., 2000; Friedlingstein et al., 2006). Furthermore, global warming could mobilize the carbon currently stored in the permafrost soil of Siberia and Central Alaska (Zimov et al., 2006; Khvorostyanov et al., 2008). Raupach and Canadell (2010) ranked such vulnerabilities of the global carbon cycle as the second largest uncertainty of the entire climate system with the largest being emissions trajectories. Independent information on the spatial and temporal pattern of CO_2 sources and sinks are needed in order to either detect the emergence of such phenomena or to test models used for projections.

ACPD
10, 18561–18605, 2010

Carbon flux and concentration measurements with a dense coverage in space and time are useful to improve our current understandings. Direct carbon flux measurements coordinated by the FLUXNET project are performed at more than 400 stations in the world (Baldocchi, 2008). The atmospheric CO_2 sampling network coordinated by the World Meteorological Organisation monitors the atmospheric carbon concentration with a precision of 0.1 ppm using surface air samples collected around the globe (e.g., GLOBALVIEW-CO_2, 2009). Using a flux inversion or so called top-down approach, the surface fluxes are derived from the spatial and temporal concentration gradients. Both the flux and surface concentration measuring networks are continuously expanding, but are nevertheless very sparse over the tropics and the oceans. In addition, they provide highly detailed information for specific locations, but their measurements are not necessarily representative of large areas. Satellite measurements provide a good spatial coverage but they are challenging because the information about the CO_2 sinks and sources located at the Earth's surface must be obtained from small variations in the column averaged mixing ratio. Several studies have evaluated the use of remotely sensed CO_2 concentrations to improve our knowledge of the spatial and temporal variability of carbon sources and sinks. Rayner and O'Brien (2001) have shown that a precision of 3 ppm or better, at monthly and 10^6 km^2 scale, is required to provide useful information on the surface fluxes. Miller et al. (2007) estimate that precisions of 1–2 ppm are necessary to monitor carbon fluxes at regional scales. Variational inversion schemes to retrieve surface fluxes have been applied to the TIROS Operational Vertical Sounder (TOVS), the Atmospheric Infrared Sounder (AIRS) and the Orbiting Carbon Observatory (OCO): While the TOVS instrument provided only little information on the carbon cycle (Chevallier et al., 2005a), AIRS observations are more precise but mostly sensitive to the upper troposphere, which makes it difficult to relate them to surface fluxes and to obtain new insights on the carbon cycle (Chevallier et al., 2005b). NASA's OCO was an instrument dedicated to make global, space-based measurements of atmospheric carbon dioxide with the precision, resolution, and coverage needed to characterize CO_2 sources and sinks on regional scales (Crisp et al., 2004). With such

ACPD
10, 18561–18605, 2010

an instrument, the error of the weekly CO_2 surface fluxes could have been reduced by up to 50% (Chevallier et al., 2007; Baker et al., 2010) and provided useful information in the tropics. OCO was lost on launch and a replacement, (OCO2) is under construction. In January 2009, the Japanese Aerospace Exploration Agency (JAXA) launched the Greenhouse Gases Observing Satellite (GOSAT), the only current space-borne mission dedicated to the measurement of atmospheric CO_2. In addition, other concepts are currently being analyzed for an improved monitoring of the carbon cycle. In particular, an active (lidar) mission could overcome some drawbacks of the OCO and GOSAT concepts. A lidar measurement would allow both day and night observations, and would be less affected by the presence of aerosol and thin clouds. The most advance concepts for a lidar based measurement of CO_2 from space are the NASA's Active Sensing of CO_2 Emissions over Nights, Days, and Seasons (ASCENDS) (Abshire et al., 2008) and the A-SCOPE mission (Ingmann, 2009) of the European Space Agency (ESA).

Houweling et al. (2004) compared the potential of SCIAMACHY, OCO, AIRS and the NOAA/CMDL flask surface network to improve CO_2 source and sink estimates obtained from inverse modelling. In this paper, an analytical inversion method is used to examine nine different observing systems and their potential combinations for the global monitoring of CO_2 surface fluxes. Besides the existing surface network, AIRS and the two CO_2 dedicated missions, OCO and GOSAT, we also include the active A-SCOPE mission and an extension of the current surface network that could be funded for the same cost as the A-SCOPE satellite. The inversion method used to derive CO_2 fluxes from concentration measurements and the different observing systems are described in Sects. 2 and 3, respectively. The results of the inter-comparison are presented in Sect. 4 and discussed in Sect. 5.

ACPD
10, 18561–18605, 2010

2 Method

An analytical inversion method (Enting, 2002) is used to infer CO_2 fluxes and their uncertainties from measured atmospheric CO_2 concentrations, an atmospheric transport model, and prior information on the fluxes. The principle relies on the definition of a-priori fluxes F_{prior} and their error covariance matrix $\mathbf{C}_{\text{prior}}$ (for a set of regions) that are further modified by the information provided by a set of atmospheric concentration measurements (O) and their error covariance matrix, $\mathbf{R}$, through a transport operator $\mathbf{H}$. Following a Bayesian framework and the assumption of Gaussian errors, the optimal fluxes, F_{post}, correspond to the minimum of the quadratic function:

$$J(F) = 1/2\left[(\mathbf{H}F - O)^{\mathrm{T}}\mathbf{R}^{-1}(\mathbf{H}F - O) + \left(F - F_{\text{prior}}\right)^{\mathrm{T}}\mathbf{C}_{\text{prior}}^{-1}\left(F - F_{\text{prior}}\right)\right]. \quad (1)$$

The transport operator $\mathbf{H}$ maps the CO_2 fluxes to the measured concentration. The solution F_{post} and the associated error covariance matrix $\mathbf{C}_{\text{post}}$ can be reached by an iterative algorithm that minimizes the cost function J (variational approach). In the case of a linear operator $\mathbf{H}$, the solution can also be obtained analytically (analytical formulation, Tarantola, 2005):

$$F_{\text{post}} = F_{\text{prior}} + \left(\mathbf{H}^{\mathrm{T}}\mathbf{R}^{-1}\mathbf{H} + \mathbf{C}_{\text{prior}}^{-1}\right)^{-1}\mathbf{H}^{\mathrm{T}}\mathbf{R}^{-1}\left(O - \mathbf{H}F_{\text{prior}}\right) \quad (2)$$

$$\mathbf{C}_{\text{post}} = \left[\mathbf{H}^{\mathrm{T}}\mathbf{R}^{-1}\mathbf{H} + \mathbf{C}_{\text{prior}}^{-1}\right]^{-1}. \quad (3)$$

Practical considerations usually guide the choice between variational and analytical approaches. In order to evaluate the potential of forthcoming observations (the objective of the study) we need to compute the posterior error covariance matrix, a quantity that does not depend on the observation values themselves but only on their error covariance matrices.

In the variational inference, the posterior error covariance matrix corresponds to the inverse of the Hessian of J at the minimum. Such calculation is usually difficult to

ACPD
10, 18561–18605, 2010

implement with either iterative or ensemble approaches. Most studies based on this approach have only estimated some elements of $\mathbf{C}_{post}$ and not the full matrix itself (Roedenbeck, 2005; Chevallier et al., 2007). On the other hand, the analytical method allows a direct computation of $\mathbf{C}_{post}$, but with potentially severe limitations linked to the sizes of the matrices to invert. Although the internal memory of computers has greatly increased in the past 20 years, making it possible to invert large matrices, there are still some limitations and the typical size of the matrices that can be easily inverted is around $10^4 \times 10^4$ elements at most. The dimension of $\boldsymbol{F}$ (and $\mathbf{C}_{post}$) is the product of the number of regions for which the fluxes are optimized by the number of time periods. With our choice of 48 time periods (8 days each) over the year, the matrix inversion constraint leads to a limitation of about 200 regions. For each region the a priori spatial distribution of the fluxes is fixed (at the resolution of the transport model) with a unique scaling coefficient in the inverse procedure. The regions were defined following the major ecosystem and climate boundaries over the continents and the different ocean basins. With the variational approach, one could relax this constraint and solve more easily for the fluxes at the resolution of the transport model (Chevallier et al., 2005b; Rödenbeck, 2005) to avoid "aggregation error" (see Kaminski et al., 2001). However there is still a debate on the optimal spatial scale at which the fluxes should be solved (e.g., Bocquet, 2005) and the performances of an inversion set up also largely depend on the structure of the prior error covariance matrix ($\mathbf{C}_{prior}$), especially the spatial and temporal correlation terms.

Given the above technical constraints, our choice of 200 regions should be seen as a compromise between optimality and feasibility. Figure 1 indicates the prior flux uncertainties used in the inversions and the region boundaries as white lines.

Over the oceans, a constant value of $0.2\,\mathrm{g\,C\,m^{-2}\,d^{-1}}$ is assumed for the uncertainty. Over land, the uncertainty is defined from the annual ecosystem respiration field of the global carbon cycle model ORCHIDEE (Krinner et al., 2005), scaled to obtain a global total uncertainty around $4\,\mathrm{Gt\,C\,yr^{-1}}$ (classical approach). At a weekly resolution, errors on any prior fluxes are likely to be correlated in time. We thus added exponentially

ACPD
10, 18561–18605, 2010

decreasing temporal correlations in $\mathbf{C}_{\text{prior}}$, with a decay time of four weeks. Given the relatively large size of each region, we did not impose spatial correlations between them. Accounting for the temporal correlations, we obtain a total land/ocean uncertainty of 4.4/0.6 Gt C yr^{-1}.

To evaluate the benefit of several observation networks including satellite instruments and potential surface networks described in Sect. 3, we will compute and compare the different error estimates ($\mathbf{C}_{\text{post}}$). More precisely, a typical error reduction (from the prior error $\mathbf{C}_{\text{prior}}$) will be analysed for specific spatial and temporal scales The impact of combinations of observing systems is also analyzed. Note that with our analytical approach Eq. (1), we can easily combine two observation networks, ($\boldsymbol{O}1$, $\mathbf{R}1$) and ($\boldsymbol{O}2$, $\mathbf{R}2$), if there is no error correlations between the observations of the two networks (i.e. $\mathbf{R}1$ and $\mathbf{R}2$ are independent). The product $[\mathbf{H}^{\mathrm{T}}\mathbf{R}^{-1}\mathbf{H}]$ can be calculated separately for each observing system and then added.

The LMDZ transport model is used to compute the sensitivity of the concentrations to the surface fluxes of the 200 regions and 48 time periods (4 periods per month). The model is derived from the general circulation model of the Laboratoire de Météorologie Dynamique (LMDZ) (Sadourny and Laval, 1984, Hourdin et al., 2006) with a spatial resolution of 3.75° (longitude) and 2.5° (latitude) with 19 vertical levels. The 3-D concentration fields (i.e. 96×73×19) were saved at each 6-h time step. In a second step, we extracted the results for each observing system described in the following section.

3 Observing systems

In this section, the nine observing systems to monitor atmospheric CO_2 concentrations, which are considered in this study, are described. These include,

- The current network of surface stations.
- The AIRS instrument onboard the Aqua satellite (Aumann et al., 2003).

ACPD
10, 18561–18605, 2010

- The SCIAMACHY instrument onboard the ENVISAT satellite (Bovensmann et al., 1999).
- The GOSAT satellite, which was launched in January 2009 (Kuze et al., 2009).
- The OCO satellite, which was lost during launch in February 2009 and is currently planned for rebuild (Crisp et al., 2004).
- The A-SCOPE mission, based on a lidar system that has been considered by the ESA but eventually not selected (Ingmann, 2009).
- Two extensions of the current surface network, named HYPOSURF-A and HYPOSURF-B, that could be build with the same funding as the A-SCOPE mission.

For each of these systems, three kinds of information are required as input to the atmospheric transport inversions: The sampling (i.e. date, time, latitude and longitude), the vertical weighting function (or averaging kernel) that quantifies the vertical sensitivity of the observation, and a realistic estimate of the measurement uncertainty. The details of each topic are described in the remainder of this section.

3.1 Sampling

First, the method used to generate a realistic sampling for both the in-situ and satellite observations is described. The current ground network consists of more than 100 stations scattered around the world. Some sample the concentrations at weekly, bi-weekly or monthly intervals, but there is a growing number of continuously measuring stations, both in Europe and North America. However, it is clear that the many measurements that are acquired on a given day cannot be considered as independent. In addition, during the night and early morning, the low atmosphere is generally very stable so that surface fluxes are trapped in the first meters above ground and the measurements are representative of a very small area only. Night-time measurements are not useable

ACPD
10, 18561–18605, 2010

by current global scale inversions. For this reason, we consider that surface stations provide one independent measurement per day, during the afternoon. The measurements acquired from high towers are less affected by the night-time trapping and are representative of a larger area. They are therefore of higher value for the monitoring of carbon fluxes and we assume that they provide four independent measurements per day, evenly distributed throughout the 24 h period (03, 09, 15, 21 local time).

Besides the existing surface network, two hypothetical network extensions that could be financed for the same price as a new satellite mission like A-SCOPE (~200 Million Euros), are considered in this study. For the hypothetical network HYPOSURF-A, the money would be invested in the construction and maintenance of 418 new continuous surface stations, using 41 already existing but currently un-instrumented towers. The second possible hypothetical network (HYPOSURF-B) would consist of towers only. In total, 168 stations could be financed, including 131 new towers and 38 currently existing towers being instrumented. The location of these potential stations were defined with the objective of an homogeneous coverage, but accounting for the ease of access determined by the presence of a weather station.

Regarding satellite measurements, a rough description of the potential sampling can be obtained with a simple orbit geometry routine, accounting for the satellite altitude and the instrument scan angles. In addition, the cloud cover has to be taken into account, because the techniques used can only measure in a cloud-free atmosphere. Using the MODIS Level 2 cloud mask (1 km resolution) of the year 2005, the presence of clouds in the field of view (FOV) was assessed for each potential sample generated by the orbitography routine (date and location). The potential observation is set as cloud contaminated and not used further whenever there is one or more cloudy MODIS pixels in the FOV. Hence, the number of clear-sky measurements depends on the instrument field of view as the probability of cloud presence increases with the FOV size.

The satellite observations can be rather dense and provide many observations per model grid box and per time-step. These observations cannot be considered as

ACPD
10, 18561–18605, 2010

independent in the inversion system because of the large correlations among their errors and among the errors of the model that simulates them. Therefore, we apply a further sampling of the observation: For each satellite orbit, we kept only the best observation of each model grid box, even when many are available. As a result of this process, we have a set of (date, lat, lon) for each observing system. A typical coverage for a month of observations is shown in Fig. 2.

3.2 Vertical weighting function

For the in-situ measurements, it is assumed that the observation is representative of the model layer corresponding to the station's altitude. For surface stations, it is the lowermost layer in most cases, with a few exceptions over hilly terrain. Airborne samples are used at the flight level. In case of towers, a typical height of 200 m is added to the station's altitude.

Satellite measurements are more difficult to handle, because the measured CO_2 concentration represents a weighted average over the whole vertical column. In general, the vertical weighting function, $w(P)$, is used to compute the column weighted average, $\overline{CO_2}$, from the concentration profile $CO_2(P)$ provided by the transport model:

$$\overline{CO_2} = \int_0^{P_{surf}} w(P) \cdot CO_2(P)\, dP\,, \tag{4}$$

where P is the atmospheric pressure. These weighting functions, derived from radiative transfer simulations, depend on several geophysical parameters such as the temperature profile, the surface albedo, or the presence of aerosol particles, as well as the observing geometry. However, for typical conditions (i.e. excluding the marginal cases with high aerosol contents or very low surface reflectances), the variations are relatively small. For the sake of simplicity, a constant weighting function is used for each of the remote sensing instruments here. They are shown in Fig. 3.

ACPD
10, 18561–18605, 2010

SCIAMACHY, OCO and GOSAT (not shown) are based on the same measurement principle (i.e. differential absorption spectroscopy) and show very similar weighting functions, with some differences that result from the spectral resolution. In all three cases, the weighting function is fairly constant throughout the troposphere, and decreases in the higher levels of the atmosphere. As a consequence, these instruments may provide a concentration estimate that is close to the tropospheric average. The weighting function from thermal infrared instruments (such as AIRS or IASI) is very different, as can be seen in Fig. 3. It peaks between 200 and 300 hPa and the relative contribution of the lower half of the atmosphere (below 500 hPa) is only on the order of 15%. Active sensing systems are also based on the differential absorption techniques but use a single pair of wavelengths only. The weighting function depends very much on the absorbing channel wavelength. For CO_2, the weak absorption band at 1.6 µm and the strong absorption band at 2.0 µm turned out to be appropriate (Koch et al., 2004; Joly et al., 2009). The weighting function at 1.6 µm peaks at 300 hPa, albeit with a significant contribution from all levels down to the surface, while the weighting function at 2.0 µm is almost proportional to the pressure. For the monitoring of surface fluxes, the latter appears most favourable, as it is the most sensitive to the atmospheric boundary layer where local surface fluxes have the largest impact. In our study, both possibilities are investigated. To distinguish them, the terms A-SCOPE-2.0 (operating at 2 µm) and A-SCOPE-1.6 (λ=1.6 µm) are used.

3.3 Measurement uncertainty

The measurement uncertainty, or error, is also a critical parameter to assess the potential impact of an observing system. The measurement uncertainty concerns the difference between simulated and observed quantities and thus contains errors in both atmospheric transport and satellite retrieval. The uncertainty is difficult to determine before real data becomes available and past experience has shown that the actual products do not always have the expected level of precision (Houweling et al., 2005). To assess the errors of the various satellite systems, we rely on radiative transfer

ACPD
10, 18561–18605, 2010

simulations performed by various groups in the context of an ESA-funded study (Bréon et al., 2009) analyzing the impact of both instrument noise and geophysical parameters. For missions using the differential absorption technique, both passive and active, the surface reflectance is a key parameter. Over the oceans, we used the statistics of glint reflectances derived from POLDER observations (Bréon and Henriot, 2006) and we accounted for the observation geometry. Over land, we used the MODIS albedo product, which is a good approximation of the reflectance for typical viewing conditions. For the particular case of A-SCOPE, the albedo was multiplied by a factor of 2, because the backscatter (or Hot-Spot) effect has to be taken into account for the lidar viewing geometry (Bréon et al., 2002).

For AIRS, it was found that the random error is mostly a function of latitude (related to the atmospheric temperature profile). Radiative transfer simulations indicate that the error on the column weighted CO_2 is close to 2.3 ppm in the tropics and strongly increases towards the polar regions. For our study, we make a simple approximation for the error σ_{AIRS}:

$$\sigma_{\mathrm{AIRS}} = 2.3 + 4 \cdot (\mathrm{lat}/90)^2 \quad [\mathrm{ppm}]. \tag{5}$$

For OCO, radiative transfer simulations indicate that the error varies with the sun and/or viewing zenith angle, the aerosol optical depth and the surface reflectance. In short, the instrument performance is best for a high reflectance, while the presence of aerosol generates some noise, especially if the atmospheric path is long. Based on a large number of simulations with varying conditions (observing geometry, surface and atmospheric conditions), the following formula was derived

$$\sigma_{\mathrm{OCO}} = 0.6 + 0.1 \cdot m\tau_{\mathrm{aer}}/\mathrm{Alb}_{1.6} \quad [\mathrm{ppm}]. \tag{6}$$

The parameter m is the airmass ($m = \cos(\theta_s)^{-1} + \cos(\theta_v)^{-1}$) which is a function of the solar zenith angle (θ_s) and the viewing angle (θ_v). τ_{aer} is the aerosol optical thickness and $\mathrm{Alb}_{1.6}$ is the surface albedo at 1.6 µm.

ACPD
10, 18561–18605, 2010

SCIAMACHY uses the same measurement technique as OCO, but with a larger random error due to its poor spectral resolution and signal-to-noise ratio. Therefore, the same formula as for OCO, but with coefficients twice as large, is used here:

$$\sigma_{\mathrm{SCIA}} = 1.2 + 0.2 \cdot m\tau_{\mathrm{aer}}/\mathrm{Alb}_{1.6} \quad [\mathrm{ppm}]. \tag{7}$$

For GOSAT, uncertainty estimates provided by the algorithm development team and discussed in Chevallier et al. (2009) describe the error as a function of the albedo and the viewing angle:

$$\sigma_{\mathrm{GOSAT}} = \sqrt{\left(\frac{0.26}{\mathrm{Alb}_{1.6}\cos\theta_s}\right)^2 + 1.2^2} \quad [\mathrm{ppm}]. \tag{8}$$

ASCOPE's measurement technique has the advantage that the error does not depend on the presence of aerosol or the sun angle. Besides, the viewing geometry is limited to nadir viewing. The main variable to define the error is the surface reflectance. Radiative transfer simulations indicate that, for a lidar working at 1.6 µm, the typical error can be fitted by:

$$\sigma_{\mathrm{ASCOPE\_1.6}} = \sqrt{(0.35 - 1.25\,\mathrm{Back}_{1.6})^2 + 0.181} \quad [\mathrm{ppm}]. \tag{9}$$

The lidar backscatter ($\mathrm{Back}_{1.6}$) is derived from the scene reflectance through a simple division by π (reflectance to backscatter). To obtain an error estimate for a lidar at 2 µm, we simply multiply the 1.6 µm error by a factor of two. This factor of 2 is consistent with the results of an extended error analysis (see Bréon et al., 2009) and allows comparing the impact of weighting function and random error (see Sect. 4).

Transport model errors are not considered for the satellite observing systems here. A recent study of Houweling et al. (2010) shows that these model errors are an important factor limiting the accuracy of the determination of CO_2 fluxes.

In-situ observations are much more precise than satellite products. Typical precision levels of 0.1 ppm can be achieved with regular calibration. On the other hand, the in-situ

measurements may not be representative of CO_2 concentration at the model grid scale used for the inversion. Also, vertical transport is more variable among transport models (Gurney et al., 2002) and probably more error-prone. It will likely impact simulations of one level at the surface more than weighted vertical integrals. Atmospheric transport simulations at high spatial resolution showed that the sub-grid variability depends very much on the location and is largest close to major CO_2 sources and sinks. Following Roedenbeck (2005), and based on high-resolution simulations, we set an error that depends on the site:

- Remote sites (islands, deserts, Antarctica): 1.0 ppm
- Shore sites with mixed Ocean/continent influence: 1.5 ppm
- Continental site with complex circulation and fluxes: 3.0 ppm
- Mountain site (on continents); simpler circulation: 1.5 ppm.

The error associated with each station can be seen in Fig. 2a.

4 Results

21 observing systems have been tested. Besides the 9 single observing systems listed in Sect. 3, we also considered eight combinations of the existing surface network with one satellite, and four combinations of the existing surface network, AIRS and one other satellite.

The analytical flux inversion yields the posterior uncertainty (σ_i) for each week and region over one year, together with the correlation terms. Since there is no reason to focus on one particular week i, we first discuss the quadratic-mean weekly error, defined as

$$\bar{\sigma}_{\text{week}} = \sqrt{\frac{1}{N}\sum_i \sigma_i^2}, \quad (10)$$

ACPD
10, 18561–18605, 2010

where N is the number of periods. Another option would be the mean weekly error, but the quadratic mean defined in Eq. (10) gives more weight to the periods with the largest uncertainties, i.e. when there is significant knowledge to be gained. Applying Eq. (10) to the prior and the posterior uncertainty, the typical weekly error reduction ER_{week} is obtained by

$$ER_{week} = 1 - \frac{\bar{\sigma}^{post}_{week}}{\bar{\sigma}^{prior}_{week}}. \quad (11)$$

The error reduction takes values between 0 and 1. High values indicate that the considered observing system is well suited to improve our knowledge on the CO_2 surface fluxes over the considered region. For each observing system simulation experiment (OSSE) we will concentrate on a few major characteristics of the posterior error covariance matrix. First, the number of observations for the different observing systems are analysed in Sect. 4.1. The typical weekly error reduction maps are then discussed in Sect. 4.2 while the posterior annual flux uncertainties are shown in Sect. 4.3. For a few regions, Table 1 provides the results (prior and posterior uncertainties, error reduction) for all 21 OSSEs. The five regions that were selected for Table 1 are France, Europe, Siberia, Tropical South America and North Atlantic. France and Europe were selected for the dense surface network over Western Europe. Siberia and South America are areas of concern with regard to climate change with very limited in-situ monitoring in South America. For ocean, we choose the North Atlantic north of 30° N, a region where recent observations suggest a significant decrease of the annual carbon sink. The analytic method makes it possible to combine the statistical results for areas that aggregate several of the pre-defined 200 regions. It is then possible to analyze how the uncertainties (or the error reduction) vary with the spatial scale. In Table 1, France, as a sub-area of Europe, can be used for that purpose. Except for France, the regions in Table 1 are based on the aggregation of several of the original 200 regions as their scale was judged representative of the processes of interest. Their dimensions are illustrated in Fig. 5d.

ACPD
10, 18561–18605, 2010

It is necessary to stress that the posterior errors and error reductions depend on many hypothesis, in particular regarding the prior flux uncertainties, their spatial and temporal covariances, and the choice of the 200 "eco-regions" that are assumed homogeneous in terms of CO_2 flux errors. Hence, we have more confidence in the relative performance of the various observing systems that are analyzed than in the absolute values (see discussion Sect. 5.1).

4.1 Number of observations

The total number of observations during the whole year varies between 26 000 (existing surface network) and 928 000 (AIRS). The geographical distribution of the existing surface stations and the pseudo-observations obtained by A-SCOPE, OCO and AIRS in January are displayed in Fig. 2. Although the surface network measurements have a high temporal resolution, the spatial coverage is much poorer compared to the satellite observations. As can be seen in Fig. 2, the sampling is very limited over South America, Africa and tropical Asia. On the contrary, A-SCOPE and AIRS result in the best global coverage because they are able to perform measurements during day and night. In contrast, no OCO measurements are possible in the high latitudes of the Northern Hemisphere in January. The same is true for SCIAMACHY and GOSAT (not shown). AIRS has the best global coverage both because it has wide scanning capabilities and because it is not affected by low clouds.

4.2 Weekly fluxes

Global maps of the typical weekly error reduction (see Eq. 10) for four OSSEs, namely the existing surface network (EXISTSURF), A-SCOPE-2.0, OCO and AIRS are shown in Fig. 4. Table 1 provides the weekly fluxes of all 21 OSSEs for four large regions (Europe, Siberia, South America and North Atlantic) which are the sum of several individual regions.

ACPD
10, 18561–18605, 2010

As expected, all observing systems provide information on the carbon fluxes and this information leads to an error reduction on the weekly fluxes. For the current surface network, the error reduction is the largest in regions with a dense coverage (Western Europe, North-eastern US and Korea-Japan). Note the white circles in Fig. 4 that show the location of the stations. In such areas, the error reduction is larger than 80%. In a small region like France (Table 1), the surface network results in the highest error reduction (87%) of all observing systems but, as the area increases (e.g. from France to Europe, Table 1), a higher error reduction is achieved by all satellite measurements, except AIRS. For other vegetated areas with a sparser surface network, the error reduction is on the order of 50%. Over continents such as Africa or South-America that are very sparsely covered, the error reduction is even lower. Over the oceans, the surface observing network provides limited information to improve the knowledge on the carbon fluxes.

Among the satellite systems, the A-SCOPE instrument provides the best constraint on surface carbon fluxes. The obtained error reductions are larger than 75% over vegetated areas and reach values between 30% and 50% over the oceans. OCO shows similar performance to the lidar mission over the tropics, but somewhat lower over the high latitudes, probably because of a lack of measurements during winter. In spite of the good spatial coverage of the AIRS instrument (Fig. 2), the error reduction of this system is much smaller than that of A-SCOPE and OCO. The reason is the higher measurement uncertainty, especially outside the Tropics, and the vertical weighting function, which is not sensitive enough to the atmospheric boundary layer and therefore weakly related to the surface fluxes.

As can be seen in Table 1, the hypothetical network extension HYPOSURF- A gives the highest error reduction of all observing systems for Europe, Siberia, South America and the North Atlantic. HYPOSURF-B results in the second highest error reduction in Europe and Siberia. The posterior uncertainties are around $0.05\,\mathrm{g\,C\,m^{-2}\,d^{-1}}$ for both cases. Note that the low error reduction (high posterior uncertainty) in the cases of HYPOSURF-A and B for France is related to the assumption that both cases are

ACPD
10, 18561–18605, 2010

possible extensions of the current network (they do not include the current network). With already a high density over Western Europe for the current network few new stations are thus foreseen over this area. If the existing surface network is combined with each hypothetical extension, the maximal error reduction of all observing systems is reached for Europe, Siberia and the North Atlantic. Hence, both hypothetical network extensions are a promising strategy for CO_2 monitoring to be compared against satellite investment (see discussion below).

Inter-comparing the error reduction of the different satellites considered in our study shows that both A-SCOPE cases are performing best, followed by OCO. The error reduction for GOSAT and SCIAMACHY are already significantly lower. The lowest error reduction was found for AIRS, except in the tropics where AIRS results in a better error reduction than GOSAT. For the two A-SCOPE cases similar error reductions are obtained in France, Europe and Siberia. For South America, A-SCOPE-1.6 is better than A-SCOPE-2.0. In general, the better weighting function of A-SCOPE-2.0 (peaked towards the surface) is compensated by the better precision of A-SCOPE-1.6. Over South America, atmospheric convection mixes the air on a deep layer. As a consequence, the weighting function of A-SCOPE-2.0 is less of an advantage, and the better precision of A-SCOPE-1.6 drives the overall performance.

Combining the measurements of one satellite with the surface network increases the total error reduction in areas with surface stations (Table 1). E.g., an error reduction of 89.6% is obtained for the combination of A-SCOPE and EXISTSURF for France. This is higher compared to the error reduction of 80.6% and 86.9% obtained for A-SCOPE and EXISTSURF as individual observing systems. As expected, the combination does not result in a higher error reduction in a region like South America where no surface measurements are available. In this case, the posterior uncertainties and the error reductions are the same as when using the satellite measurements alone. Table 1 also shows that the additional consideration of AIRS does not improve the results obtained over Europe and Siberia for the combination of the existing surface network with A-SCOPE, OCO and GOSAT, respectively. AIRS adds some information only in

ACPD
10, 18561–18605, 2010

the Tropics. Again, this is understood as the effect of deep convection that links the surface and the mid and upper troposphere which AIRS is sensitive to.

To investigate the advantages and disadvantages of the different observing systems, it is also interesting to look at the change of the performance within one year. Therefore, time series of the monthly error reduction (accounting for covariances between weekly errors) for the existing surface network, A-SCOPE-2.0, OCO and AIRS are shown in Fig. 5. We observe significant seasonal variations for the four selected regions that reflect seasonal variations of the prior errors, of the number of observations, and of seasonal variations in the atmospheric vertical mixing (probably more crucial for the surface networks). Altogether, A-SCOPE is performing best, with the highest error reduction for all regions, except France where the existing surface network dominates, and with the smallest monthly variations. In the case of South America, Fig. 5 emphasises the very good performance of OCO throughout the year, while the surface network shows low error reduction and a seasonal pattern linked to changes in atmospheric mixing. For Europe and Siberia, the monthly error reduction of OCO in the summer months is almost as high as the one for A-SCOPE. The strong annual cycle in the error reduction for these two regions reflects that of the prior uncertainties (larger flux uncertainties in summer) modulated by the number of measurements of each observing system. In winter the lidar-based A-SCOPE mission provides more information than OCO's because the sun is too low to permit measurements by the passive technique of the OCO mission. As already seen, AIRS's performance is only competitive with the other satellites in South America. In other regions, the performance is significantly worse than that of the other satellite systems, and shows an annual cycle that reflects the prior uncertainties.

4.3 Annual fluxes

Posterior errors of annual fluxes are given in Fig. 6 (mapping of the annual error of the 200 regions). With the existing surface network posterior errors smaller than $20\,\mathrm{g\,C\,m^{-2}\,yr^{-1}}$ are reached over land where stations are available (a few regions

ACPD
10, 18561–18605, 2010

in Europe and North America). In these regions, e.g., France, none of the satellite systems attains such a low posterior uncertainty (see numbers in Table 1). On the other hand, the posterior uncertainty of the existing surface network amounts to more than 45 g C m^{-2} yr^{-1} in South America, Siberia and Southern Africa, and around 15 g C m^{-2} yr^{-1} over the ocean. Over vegetated areas the A-SCOPE posterior error is in the range of 10 to 30 g C m^{-2} yr^{-1}. In most ocean regions the uncertainty is below 10 g C m^{-2} yr^{-1}. For OCO the posterior errors are slightly larger with values between 15 and 50 g C m^{-2} yr^{-1} over land and up to 15 g C m^{-2} yr^{-1} over the oceans.

Annual flux errors for larger regions (i.e. aggregation of few individual regions) such as Europe, Siberia, South America and the North Atlantic are also given in Table 1. The computation of these errors accounts for all spatial covariances in $\mathbf{C}_{\text{post}}$ (Eq. 3). The resulting annual flux uncertainties appear to be much smaller than the uncertainty of the individual regions shown in Fig. 6. For both A-SCOPE cases, the error per unit area decreases by a factor 8–9 between France and Europe (from around 30 to 3.5 g C m^{-2} yr^{-1}). This reduction partly results from negative error correlations. Without these correlation terms the error would reduce to only 5.2 g C m^{-2} yr^{-1} as a results of aggregating regions with independent errors. The change from 5.2 to 3.5 g C m^{-2} yr^{-1} becomes important when assessing the potential of an observing system to constrain annual fluxes as a function of spatial scale (see Sect. 5.1). It highlights the importance of negative error correlations between adjacent regions. As can be seen in Table 1, an extension of the surface network is encouraging. HYPOSURF-A results in the lowest posterior error of all observing systems for Europe, Siberia and South America. A-SCOPE and OCO are much better than the other satellites. GOSAT and SCIAMACHY produce posterior errors about twice those of A-SCOPE and OCO. In South America the performance of AIRS is comparable to that of GOSAT and SCIAMACHY, while in Europe and Siberia the posterior error achieved with AIRS is around 25 and 35 g C m^{-2} yr^{-1}, respectively. The existing surface network combined with A-SCOPE significantly decreases the annual error over France (region with a dense network). The same is true for the combination of EXISTSURF with the surface network extensions.

ACPD
10, 18561–18605, 2010

For ocean, the posterior error decreases from around 7(12) $g\,C\,m^{-2}\,yr^{-1}$, for an individual region of North Atlantic (East Atlantic, Fig. 6) to around 2(3) $g\,C\,m^{-2}\,yr^{-1}$, for the whole North Atlantic (>30° N) for A-SCOPE-20 and the surface network, respectively.

5 Discussion

Before discussing the implications of our results for CO_2 observing systems in Sect. 5.2 there are several caveats which must be explored.

5.1 How robust is the comparison?

We see from Eq. (3) that the error reduction depends on the uncertainty covariances for prior flux estimates and measurements plus the matrix representing transport. The choice of source resolution is critical as it underlies the two of them.

Source resolution:
Even though we perform all OSSEs with the same set-up, the source resolution will impact the results. Our set-up, with 200 regions tiling the globe, may be viewed as not representing the current state of the art in source/sink inversions. These are usually performed at gridpoint resolution with the imposition of evanescent correlations among pixels, although few recent studies choose to resolve the fluxes for large "ecosystem regions" (i.e. CarbonTracker, Peters et al., 2007). These correlation lengths are largely unknown and, like all other aspects of the prior statistics, should be informed by independent data (e.g., Chevallier et al., 2006).

The source resolution also enters the problem via the influence or footprint of each measurement. In an inversion with fixed regions, the whole region is constrained by a single measurement while the same measurement applies a less rigid constraint using gridpoints and correlations. Given the sum of squares nature of the posterior Hessian (Eq. 3) there are sharply diminishing returns as a region is oversampled. Imagining the limiting case of infinite prior uncertainty and no transport (i.e. each measurement

ACPD
10, 18561–18605, 2010

only sees fluxes from its own region) we see that the posterior uncertainty will remain infinite for regions without a station. The number of surface stations required hence depends critically on the source resolution (and potential correlations). This dependence is much weaker for satellite measurements. As a direct consequence, we obtain for instance a larger error reduction for large ocean basins compared to smaller adjacent basins (Fig. 4), with corresponding lower posterior errors (Fig. 6).

Transport resolution:

The transport model resolution also enters the problem. The use of correlations (or large regions) avoids the dominance of the near-field noted by Bocquet (2005) and Gerbig et al. (2009). Our choice of sampling for the satellite measurements (Sect. 3.1) is, however, strongly dependent on model resolution. The implication that the high-resolution soundings of instruments like OCO or A-SCOPE contain errors with respect to the transport model completely correlated at 250 km (the approximate north-south extent of an LMDZ gridbox) and completely uncorrelated beyond this has no geophysical basis. It is most likely that there is extra information at smaller scales and that this information would strengthen the constraint offered by these instruments as resolution was increased.

The performance of the surface network is also affected by capabilities of the transport model. The term representativeness describes the extent to which a given measurement represents a model gridbox. It is different from the problem of grouping pixels into regions discussed above. Representativeness errors form part of the uncertainty covariance for data (**R** in Eqs. 2 and 3). They are likely larger for larger gridboxes and more heterogeneous sources. Corbin et al. (2009) has shown that they are not large for column-integrated measurements taken in swaths over a gridbox (a measurement reminiscent of a satellite) but the problem is less widely studied for surface measurements.

Representativeness errors will certainly decrease as model resolution increases. So, probably, will errors in transport. Geels et al. (2006) and Law et al. (2008) have both shown that higher resolution models, particularly mesoscale models, can capture much

ACPD
10, 18561–18605, 2010

more of the information available from continuous surface measurements. Inversion studies such as Lauvaux et al. (2009) have shown that this information can provide an improved constraint for surface fluxes. Initial tests (R. Engelen (ECMWF), personal communication, 2010) suggest that models running at tens of kilometers resolution could use far more than the one daily measurement from surface stations or four from towers used here, improving the performance of the surface network.

Prior flux error covariance:

The prior covariance matrix ($\mathbf{C}_{\text{prior}}$) that we have defined neglects key characteristics of the carbon cycle and should still be considered a crude approximation. Indeed, the error correlation terms are difficult to assess and are only partially accounted for in $\mathbf{C}_{\text{prior}}$. We use "eco-regions" for the spatial domain and only positive temporal correlations for the time domain (exponential decay with a time constant of one month). However, negative correlations between summer and winter flux errors for instance, are not included (an excess of carbon uptake during the growing season is likely to enhance the respiration in the following months). Omitting these terms leads to an overall prior annual land and ocean error budget of 4.4 and 0.6 Gt C yr^{-1}, respectively, which is unrealistically large for land given our knowledge of the carbon cycle. As a direct consequence, the posterior budget is likely overestimated (i.e. 0.73 and 0.47 for land and ocean with the EXISTSURF observing system). We expect this to have larger effects on the absolute errors discussed throughout the paper than the relative performance of different systems.

Data uncertainty:

The final critical input to the calculations is the data uncertainty covariance **R**. We stress again that this represents uncertainty in the model-data mismatch and so contains components from the measurement itself (already the product of an inversion procedure for satellite data), representativeness error (already described) and errors in atmospheric transport simulations. We have already commented on the implicit correlation structure in CO_2 measurement error for satellites. Along with the possibility that higher model resolution would allow more measurements we must also allow the

ACPD
10, 18561–18605, 2010

possibility that confounding influences on satellite retrievals such as aerosol and thin clouds could induce coherent errors beyond one gridbox, especially in high latitudes where gridboxes are small. This would decrease the information content of satellite data.

For the surface network the problem rests on transport error. It is generally thought that, with higher uncertainty in vertical transport, this component of model error should be larger for surface than column-integrated measurements. Our specification of **R** takes this into account but we have little way of knowing whether we have captured the difference successfully and even less of predicting how these differences will compare as models improve.

Overall, our study has a range of limitations when comparing satellite and surface systems. These may compensate or exacerbate each other, precluding an unambiguous result. Two things can be concluded firmly however. First the choice of measurement approaches depends on the quality of the tools we use to interpret them. Given all above limitations, we guess that current set-up likely favours the surface network. Second, the combination of both observing systems is likely to bring cross constraint in the optimization process and thus to decrease the impact of each system's biases and provide the most precise flux estimates. Additionally we suggest that a large surface network expansion, although probably difficult to achieve over the tropics, would require significant model improvement (representativeness and transport errors), while for the foreseen satellite instruments the precision of the measurements is crucial although still largely debated.

Concerning the rating of the different satellites, it was shown in Sect. 4, that they do not perform equally and that A-SCOPE provides the best information on the surface fluxes among them. The information provided by GOSAT is less compared to OCO or A-SCOPE and is similar to that of SCIAMACHY. This result may seems surprising considering the fact that it is a carbon-dedicated instrument, but this follows directly from the cautious precision estimates provided by the GOSAT team. This situation may well change as confidence in GOSAT retrieval algorithms grows. AIRS does a poor job for

ACPD
10, 18561–18605, 2010

providing additional information on the carbon fluxes in particular over mid and high latitude where the measurements are of much lower quality than over the tropics. The ranking of the different satellite systems is directly linked to the number of measurements, the assumed errors and the vertical weighting functions. The ranking of the satellite systems is likely to be more robust than the differences between the surface and the satellite observing systems, given the limitations discussed above.

5.2 Potential of the observing systems and carbon cycle targets

The results presented above demonstrate that all observing systems discussed in this paper may improve our knowledge of the carbon cycle. Indeed, the amplitude of the error reduction on the regional fluxes is significant and reaches values up to 90%. However, such error reduction (or more directly the posterior error) depends on the inverse set-up. Furthermore, it may be insufficient to answer key questions of the carbon cycle that may require even lower errors. The following discussion is based on the absolute posterior error rather than the error reduction and we stress again the sensitivity of this diagnostic to various inputs (see Sect. 5.1). We note that the scientific community tends to use an ensemble of inversions (varying several components) to define a more robust error diagnostic (see for instance the TransCom experiment, Gurney et al., 2003). Being aware of these limitations, it is still interesting to attempt to quantify the requirements for some key questions, and assess whether these requirements can be met by the various observing systems that we have defined. We have identified four key questions: one of them focuses on the weekly/monthly fluxes, while the other ones focus on annual fluxes. The requirements are discussed below and summarized in Table 2.

Land-Vegetation dynamics:

Vegetation dynamic models are developed to understand the functioning of ecosystems and to predict their future behaviour including their response to climate change. Measurements of the carbon fluxes are very useful to evaluate and improve vegetation

ACPD
10, 18561–18605, 2010

and soil dynamic models over large-scale areas. Typical spatial scales needed for this purpose combine the scale of the synoptic variation of atmospheric variables and the heterogeneity of the land surface cover resulting in a range between 200 km (i.e., some European ecosystems) and 1000 km (i.e. Amazonian forests). The temporal scale is between one week (target) and one month (threshold). For a temperate region and at the spatial scale defined above, CO_2 fluxes vary between $-2.5\,g\,C\,m^{-2}\,d^{-1}$ during the peak of the growing season and $+0.5\,g\,C\,d^{-1}$ during winter. Given the current uncertainties of the models (up to 50%), a realistic objective is to monitor the fluxes within 20%. Hence, it would be necessary to determine the weekly/monthly fluxes with a precision of around $0.3\,g\,C\,m^{-2}\,d^{-1}$.

Based on the weekly fluxes given in Table 1, it appears that posterior uncertainty values below $0.10\,g\,C\,m^{-2}\,d^{-1}$ are obtained for HYPOSURF-A and B, both A-SCOPE cases and OCO over Europe, Siberia and South America. The other observing systems provide posterior uncertainties that are close or below the target precison of $0.3\,g\,C\,m^{-2}\,d^{-1}$. However, this is for spatial scales that are only compatible with that of the upper limit of the requirement. Indeed, for the smaller "France" region, a posterior uncertainty better than $0.3\,g\,C\,m^{-2}\,d^{-1}$ is only reached for the combination of EXIST-SURF with A-SCOPE. A further analysis of the maps indicate that the target objective for the "vegetation dynamic" key question can only be reached for the combination of a dense surface network and a satellite such as OCO or A-SCOPE.

Vegetation feedback to climate change:

The location of the current global annual vegetation sink, which is on the order of $2\,Gt\,C\,yr^{-1}$ is not yet agreed on. One key question of the carbon cycle is to monitor the large scale sources and sinks as well as the feedback of the vegetation to climate change. Current estimates of the net carbon fluxes over various ecosystems with a typical size of $2000\times2000\,km^2$ vary between 0.2 and $1\,Gt\,C\,yr^{-1}$. There is therefore a need to measure the net carbon flux with a precision better than $0.1\,Gt\,C\,yr^{-1}$ (threshold) or 0.02 Gt C (target) at this scale. Hence, observing systems with precisions better than $25\,g\,C\,m^{-2}\,yr^{-1}$ (threshold) and $5\,g\,C\,m^{-2}\,yr^{-1}$ (target) would be needed to locate

ACPD
10, 18561–18605, 2010

the vegetation annual sources and sinks, and allow investigations of the vegetation response to climate change.

From our results, it appears that most observing systems cannot meet the target requirements (5 g C m^{-2} yr^{-1}) on the annual net carbon fluxes over land. The A-SCOPE observing system does meet that requirement over a few vegetated areas. Both A-SCOPE and OCO meet the threshold requirement (25 g C m^{-2} yr^{-1}) over a majority of land surface regions, and so do both hypothetical networks. It therefore appears difficult to properly measure the annual vegetation carbon fluxes, at the target requirements for this spatial scale (~2000 km), although the best observing systems can provide significant information. At the larger continental scale, A-SCOPE and HYPOSURF systems meet that requirement.

Ocean sink and its variations:

In the case of the oceans, ongoing debates focus not only on the annual carbon sinks over the North Atlantic (Schuster and Watson, 2007) and the Southern Ocean (Lovenduski et al., 2008; Le Quéré et al., 2009) but also on their recent trends. Current estimates of mean ocean fluxes are based on measurements of the CO_2 partial pressure (Takahashi et al., 2009). For a region of typical size 2500×2500 km^2, the net flux between the atmosphere and the ocean varies between a few g C m^{-2} yr^{-1} and 30 g C m^{-2} yr^{-1} and there is need to estimate the fluxes with 20% relative precision. Hence, a requirement of 3 g C m^{-2} yr^{-1} is defined for ocean regions in this study.

Such target requirement is much stronger than for land and none of the observing systems can meet it, at the spatial scale of the individual regions (i.e., 1500 km) At this scale the annual error are closer to 10 g C m^{-2} yr^{-1} for the favourable cases of A-SCOPE. Aggregated at larger spatial scale, we obtain annual errors on the order of 2 g C m^{-2} yr^{-1} (2.85 and 1.93 for EXISTSURF and A-SCOPE2.0, respectively) for the North Atlantic (>30° N) which becomes compatible with the requirement. The conclusion is therefore similar as that over land, that the requirements can only be met over large basin scale.

ACPD
10, 18561–18605, 2010

Anthropogenic emissions and international treaties:
A political objective for the estimation of CO_2 fluxes is the monitoring of the compliance with Kyoto-like protocols. The Kyoto protocol requests countries to decrease their CO_2 emissions by a few percent compared to 1990 levels. To verify such a commitment, over the five year life of a satellite, it appears necessary to measure the annual emissions at the 1% precision level, although a bias could be acceptable. At a scale of $500 \times 500\,km^2$, the typical anthropogenic flux of an industrialised country is about $0.1\,Gt\,C\,yr^{-1}$. A precision on the order of 1% of the net anthropogenic contribution translates into a measurement requirement of $4\,g\,C\,m^{-2}\,yr^{-1}$.

In this case, the requirements are even stronger than those for the oceanic or land fluxes as the required spatial scale is much smaller. Unsurprisingly, it appears that none of the observing systems or their combination can provide the necessary information to measure the fluxes with the required precision. However, as discussed above, the errors on the annual totals might be overestimated. On the other hand, the observation eror budget might be underestimated. Hence, additional investigations would be needed before any firm conclusion about the potential of these observing systems for the "ocean" and "anthropogenic" key questions.

This evaluation demonstrates that, although a significant improvement to carbon cycle knowledge may be expected from forthcoming surface or space-borne observing systems, they might nevertheless be insufficient to answer alone some of the key questions. Additional and complementary information will be needed, in particular to better constrain the ocean fluxes or to monitor the anthropogenic emissions as needed in the context of international treaties. Of course there is a wealth of such information available (e.g., O_2/N_2 data, land ecosystem flux measurements or forest biomass increments for certain regions.) and so a clear outcome of this analysis is the need to build systems that can integrate streams of information with the atmospheric data studied here.

ACPD
10, 18561–18605, 2010

6 Conclusion

In this study, Observing System Simulation Experiments were performed to assess the potential information content of various observing systems to constrain our knowledge of the carbon surface fluxes. The observing systems included the current observing network, a number of operational or potential satellites, two hypothetical surface networks that could be created with the same funding as a satellite, and a number of combinations of the above.

One main finding of this study is that the A-SCOPE mission provides the best information content of the various satellite systems that were studied. The information content is significantly better than that provided by OCO, in particular over mid and high latitudes and over the oceans. The A-SCOPE system allows an error reduction of the weekly fluxes of more than 80% over most vegetated areas. This number is consistent with the scientific requirements for the monitoring of vegetation dynamics. Measurements such as those provided by A-SCOPE would help the development of new models of the vegetation and its interaction with the atmosphere.

On the other hand, the posterior uncertainties on the fluxes are still too large to properly monitor anthropogenic fluxes in the context of Kyoto-like protocols. Moreover we should notice that the measurements provided by the mission would only bring constrain to the natural plus anthropogenic fluxes with no direct method to distinguish the relative contributions.

Nevertheless, the precisions appear sufficient to monitor long-term natural fluxes, such as those posited as a response to climate change, but only at the large spatial scales of subcontinents or oceanic basins. Another important finding is that, if an extension of the current surface network could be funded with the same amount of money as the satellite system, it would provide similar performance. The choice between these two is hence logistic or even political, e.g. a preference for an open internationally accessible measurement.

ACPD
10, 18561–18605, 2010

Acknowledgements. This study was supported by the European Space Agency under contract No. 20839/07/NL/HE. The authors are grateful to Paul Ingmann (ESA) and NOVELTIS, especially Pascal Prunet, for organizing the project. We would also like to thank all the project members, especially Julia Marshall (Max Planck Institute for Biogeochemistry, Jena, Germany) for providing the station lists and representativity errors of the three surface networks, Didier Bruneau (Service d'Aeronomie, Verrières, France) and Gerhard Ehret (German Aerospace Center, Oberpfaffenhofen, Germany) for the estimates of the performances of a lidar instrument. The OCO error estimate was provided by Hartmut Bösch (University for Leicester, UK). We would like to acknowledge the contribution of the CNES in the development of the analytical inversion tool used in this study (contract number DCT/SI/IM-2008-10419). This work was performed using HPC resources from GENCI – [CCRT/CINES/IDRIS] (Grant 2009-t2009012201) and from DSM [CCRT/CEA].

The publication of this article is financed by CNRS-INSU.

References

Abshire, J. B., Riris, H., Allan, G., Mao, J., Wilson, E., Stephen, M., Sun, X., Weaver, C., and Chen, J.: Laser Sounder for Measurement of CO_2 Concentrations in the Troposphere for the ASCENDS Mission – Progress, Earth Science Technology Conference (ESTC), 2008.

Aumann, H. H., Chahine, M. T., Gautier, C., Goldberg, M. D., Kalnay, E., McMillin, L. M., Revercomb, H., Rosenkranz, P. W., Smith, W. L., Staelin, D. H., Strow, L. L., and Susskind, J.: AIRS/AMSU/HSB on the Aqua mission: Design, science objectives, data products, and processing systems, IEEE T. Geosci. Remote, 41(2), 253–264, 2003.

Baldocchi, D.: Breathing of the terrestrial biosphere: Lessons learned from a global network of carbon dioxide flux measurement systems, Aust. J. Bot., 56(1), 1–26, 2008.

ACPD
10, 18561–18605, 2010

Baker, D. F., Bösch, H., Doney, S. C., O'Brien, D., and Schimel, D. S.: Carbon source/sink information provided by column CO_2 measurements from the Orbiting Carbon Observatory, Atmos. Chem. Phys., 10, 4145–4165, doi:10.5194/acp-10-4145-2010, 2010.

Bocquet, M.: Grid resolution dependence in the reconstruction of an atmospheric tracer source, Nonlinear Proc. Geoph., 2, 219–233, 2005.

Bovensmann, H., Burrows, J. P., Buchwitz, M., Frerick, J., Noël, S., Rozanov, V., Chance, K. V., and Goede, A. P. H.: SCIAMACHY: Mission objectives and measurement modes, J. Atmos. Sci., 56, 127–150, 1999.

Bréon, F. M., Houweling, S., Marshall, J., Chevallier, F., Flamant, P., Ehret, G., Bruneau, D., and Prunet, P.: Observation techniques and mission concepts for the analysis of the carbon cycle, Final report of ESA Contract No. 20839/07/NL/HE, 2009.

Bréon, F.-M., Maignan, F., Leroy, M., and Grant, I.: Analysis of hot spot directional signatures measured from space, J. Geophys. Res., 107(D16), 4282, doi:10.1029/2001JD001094, 2002.

Bréon, F.-M. and Henriot, N.: Spaceborne observations of ocean glint reflectance and modeling of wave slope distributions, J. Geophys. Res., 111, C06005, doi:10.1029/2005JC003343, 2006.

Canadell, J. G., Le Quéré C., Raupach, M. R., Field, C. B., Buitenhuis, E. T., Ciais, P., Conway, T. J., Gillett, N. P., Houghton, R. A., and Marland, G.: Contributions to accelerating atmospheric CO_2 growth from economic activity, carbon intensity, and efficiency of natural sinks, PNAS, 104(47), 18866–18870, 2007.

Chevallier, F., Fisher, M., Peylin, P., Serrar, S., Bousquet, P., Bréon, F.-M., Chédin, A., and Ciais, P.: Inferring CO_2 sources and sinks from satellite observations: method and application to TOVS data, J. Geophys. Res., 110, D24309, doi:10.1029/2005JD006390, 2005a.

Chevallier, F., Engelen, R. J., and Peylin, P.: The contribution of AIRS data to the estimation of CO_2 sources and sinks, Geophys. Res. Lett., 32, L23801, doi:10.1029/ 2005GL024229, 2005b.

Chevallier, F., Viovy, N., Reichstein, M., and Ciais, P.: On the assignment of prior errors in Bayesian inversions of CO_2 surface fluxes, Geophys. Res. Lett., 33, L13802, doi:10.1029/2006GL026496, 2006.

Chevallier, F., Bréon, F.-M., and Rayner, P. J.: The contribution of the Orbiting Carbon Observatory to the estimation of CO_2 sources and sinks: Theoretical study in a variational data assimilation framework, J. Geophys. Res., 112, D09307, doi:10.1029/2006JD007375, 2007.

ACPD
10, 18561–18605, 2010

Chevallier, F., Maksyutov, S., Bousquet, P., Bréon, F.-M., Saito, R., Yoshida, Y., and Yokota, T.: On the accuracy of the CO_2 surface fluxes to be estimated from the GOSAT observations, Geophys. Res. Lett., 36, L19807, doi:10.1029/2009GL040108, 2009.

Corbin, K. D., Denning, A. S., and Parazoo, N. C.: Assessing temporal clear-sky errors in assimilation of satellite CO_2 retrievals using a global transport model, Atmos. Chem. Phys., 9, 3043–3048, doi:10.5194/acp-9-3043-2009, 2009.

Cox, P. M., Betts, R. A., Jones, C. D., Spall, S. A., and Totterdell, I. J.: Acceleration of global warming due to carbon-cycle feedbacks in a coupled climate model, Nature, 408(6809), 184–7, 2000.

Crisp, D., Atlas, R. M., Bréon, F.-M., Brown, L. R., Burrows, J. P., Ciais, P., Connor, B. J., Doney, S. C., Fung, I. Y., Jacob, D. J., Miller, C. E., O'Brien, D., Pawson, S., Randerson, J. T., Rayner, P., Salawitch, R. J., Sander, S. P., Sen, B., Stephens, G. L., Tans, P. P., Toon, G. C., Wennberg, P. O., Wofsy, S. C., Yung, Y. L., Kuang, Z., Chudasama, B., Sprague, G., Weiss, B., Pollock, R., Kenyon, D., and Schroll, S.: The orbiting carbon observatory (OCO) mission, Adv. Space Res., 34(4), 700–709, 2004.

Enting, I. G.: Inverse Problems in Atmospheric Constituent Transport, Cambridge University Press, Cambrigde, 2002.

Friedlingstein, P., Cox, P., Betts, R., Bopp, L., von Bloh, W., Brovkin, V., Cadule, P., Doney, S., Eby, M., Fung, I., Bala, G., John, J., Jones, C., Joos, F., Kato, T., Kawamiya, M., Knorr, W., Lindsay, K., Matthews, H. D., Raddatz, T., Rayner, P., Reick, C., Roeckner, E., Schnitzler, K.-G., Schnur, R., Strassmann, K., Weaver, A. J., Yoshikawa, C., and Zeng, N.: Climate carbon cycle feedback analysis: results from the C4MIP model intercomparison, J. Climate, 19(14), 3337, 2006.

Geels, C., Gloor, M., Ciais, P., Bousquet, P., Peylin, P., Vermeulen, A. T., Dargaville, R., Aalto, T., Brandt, J., Christensen, J. H., Frohn, L. M., Haszpra, L., Karstens, U., Rödenbeck, C., Ramonet, M., Carboni, G., and Santaguida, R.: Comparing atmospheric transport models for future regional inversions over Europe – Part 1: Mapping the atmospheric CO_2 signals, Atmos. Chem. Phys., 7, 3461–3479, doi:10.5194/acp-7-3461-2007, 2007.

Gerbig, C., Dolman, A. J., and Heimann, M.: On observational and modelling strategies targeted at regional carbon exchange over continents, Biogeosciences, 6, 1949–1959, doi:10.5194/bg-6-1949-2009, 2009.

GLOBALVIEW-CO_2: Cooperative Atmospheric Data Integration Project – Carbon Dioxide. CD-ROM, NOAA ESRL, Boulder, Colorado [Also available on Internet via anonymous FTP to

ACPD
10, 18561–18605, 2010

ftp.cmdl.noaa.gov, Path: ccg/co2/GLOBALVIEW], 2009.
Gruber, N. Gloor, M., Mikaloff Fletcher, S. E., Doney, S. C. et al.: Oceanic sources, sinks, and transport of atmospheric CO_2, Global Biogeochem. Cy., 23, GB1005, doi:10.1029/2008GB003349, 2009.
Gurney, K. R., Law, R. M., Denning, A. S., Rayner, P. J., Baker, D. et al.: Towards robust regional estimates of CO_2 sources and sinks using atmospheric transport models, Nature, 415, 626–630, 2002.
Gurney, K. R., Law, R. M., Denning, A. S., Rayner, P. J., Baker, D., Bousquet, P., Bruhwiler, L., Chen, Y. H., Ciais, P., Fan, S. et al.: TransCom 3 CO_2 inversion intercomparison: 1. Annual mean control results and sensitivity to transport and prior flux information, Tellus B, 55(2), 555–579, 2003.
Hourdin, F., Musat, I., Bony, S., Braconnot, P., Codron, F., Dufresne, J., Fairhead, L., Filiberti, M., Friedlingstein, P., Grandpeix, J., Krinner, G., LeVan, P., Li, Z., and Lott, F.: The LMDZ4 general circulation model: Climate performance and sensitivity to parametrized physics with emphasis on tropical convection, Clim. Dynam., 27, 787–813, 2006.
Houweling, S., Bréon, F.-M., Aben, I., Rödenbeck, C., Gloor, M., Heimann, M., and Ciais, P.: Inverse modeling of CO_2 sources and sinks using satellite data: A synthetic inter-comparison of measurement techniques and their performance as a function of space and time, Atmos. Chem. Phys., 4, 523–538, doi:10.5194/acp-4-523-2004, 2004.
Houweling, S., Hartmann, W., Aben, I., Schrijver, H., Skidmore, J., Roelofs, G.-J., and Bréon, F.-M.: Evidence of systematic errors in SCIAMACHY-observed CO_2 due to aerosols, Atmos. Chem. Phys., 5, 3003–3013, doi:10.5194/acp-5-3003-2005, 2005.
Houweling, S., Aben, I., Breon, F.-M., Chevallier, F., Deutscher, N., Engelen, R., Gerbig, C., Griffith, D., Hungershoefer, K., Macatangay, R., Marshall, J., Notholt, J., Peters, W., and Serrar, S.: The importance of transport model uncertainties for the estimation of CO_2 sources and sinks using satellite measurements, Atmos. Chem. Phys. Discuss., 10, 14737–14769, doi:10.5194/acpd-10-14737-2010, 2010.
Ingmann, P.: A-SCOPE, Advanced Space Carbon and Climate Observation of Planet Earth, Report of Assessment, SP-1313/1, ESA Communication Product Office, Noordwijk, The Netherlands, 2009
IPCC: Climate Change 2007 – The Physical Science Basis. Contribution of Working Group I to the Fourth Assessment Report of the IPCC, Cambridge University Press, 2007.
Joly, L., Marnas, F., Gibert, F., Bruneau, D., Grouiez, B., Flamant, P. H., Durry, G., Dumelie, N.,

ACPD
10, 18561–18605, 2010

Parvitte, B., and Zéninari, V.: Laser diode absorption spectroscopy for accurate CO_2 line parameters at 2 mm: Consequences for space-based DIAL measurements and potential biases, Appl. Optics, 48(29), 5475–5483, 2009.

Law, R. M., Peter, W., Rödenbeck, C., Aulagnier, C. et al.: TransCom model simulations of hourly atmospheric CO_2: Experimental overview and diurnal cycle results for 2002, Gobal Biogeochem. Cy., 22, GB3009, doi:10.1029/2007GB003050, 2008.

Lauvaux, T., Pannekoucke, O., Sarrat, C., Chevallier, F., Ciais, P., Noilhan, J., and Rayner, P. J.: Structure of the transport uncertainty in mesoscale inversions of CO_2 sources and sinks using ensemble model simulations, Biogeosciences, 6, 1089–1102, doi:10.5194/bg-6-1089-2009, 2009.

Kaminski, T., Rayner, P., Heimann, M., and Enting, I.: On aggregation errors in atmospheric transport inversions, J. Geophys. Res., 106(D5), 4703, 2001.

Khvorostyanov, D. V., Ciais, P., Krinner, G., and Zimov, S. A.: Vulnerability of East Siberia's frozen carbon stores to future warming, Geophys. Res. Lett., 35, L10703, doi:10.1029/2008GL033639, 2008.

Koch, G. J., Barnes, B. W., Petros, M., Beyon, J. Y., Amzajerdian, F., Yu, J., Davis, R. E., Ismail, S., Vay, S., Kavaya, M. J., and Singh, U. N.: Coherent differential absorption lidar measurements of CO_2, Appl. Optics, 43(26), 5092–5099, doi:10.1364/AO.43.005092, 2004.

Krinner, G., Viovy, N., de Noblet-Ducoudré, N., Ogée, J., Polcher, J., Friedlingstein, P., Ciais, P., Sitch, S., and Prentice, I. C.: A dynamic global vegetation model for studies of the coupled atmosphere-biosphere system, Global Biogeochem. Cy., 19, GB1015, doi:10.1029/2003GB002199, 2005.

Kuze, A., Suto, H., Nakajima, M., and Hamazaki, T.: Thermal and near infrared sensor for carbon observation Fourier-transform spectrometer on the Greenhouse Gases Observing Satellite for greenhouse gases monitoring, Appl. Optics, 48(35), 6716–6733, doi:10.1364/AO.48.006716, 2009.

Le Quéré, C., Rodenbeck, C., Buitenhuis, E. T., Conway, T. J., Langenfelds, R., Gomez, A., Labuschagne, C., Ramonet, M., Nakazawa, T., Metzl, N., Gillett, N., and Heimann, M.: Saturation of the southern ocean CO_2 sink due to recent climate change, Science, 316(5832), 1735–1738, 2007.

Le Quéré, C., Raupach, M. R., Canadell, J. G., Marland, G. et al.: Trends in the sources and sinks of carbon dioxide, Nat. Geosci., 2, 831–836, doi:10.1038/ngeo689, 2009.

Lovenduski, N. S., Gruber, N., and Doney, S. C.: Toward a mechanistic understanding of the

ACPD
10, 18561–18605, 2010

decadal trends in the Southern Ocean carbon sink, Global Biogeochem. Cy., 22, GB3016, doi:10.1029/2007GB003139, 2008.

Miller, C. E., Crisp, D., DeCola, P. L., Olsen, S. C., Randerson, J. T. et al.: Precision requirements for space-based XCO_2 data, J. Geophys. Res., 112, D10314, doi:10.1029/2006JD007659, 2007.

Peters, W., Jacobson, A. R., Sweeney, C., Andrews A. E. et al.: An atmospheric perspective on North American carbon dioxide exchange: CarbonTracker, PNAS, 104(48), 18925–18930, doi:10.1073/pnas.0708986104, 2007.

Raupach, M. R. and Canadell, J. G.: Carbon and the Anthropocene, Current Opinion in Environmental Sustainability, Current Opinion in Environmental Sustainability, In Press, Corrected Proof, Available online 8 June 2010, ISSN 1877–3435, doi:10.1016/j.cosust.2010.04.003, 2010.

Rayner, P. J. and O'Brien, D. M.: The utility of remotely sensed CO_2 concentration data in surface source inversions, Geophys. Res. Lett., 28(1), 175–178, 2001.

Rödenbeck, C.: Estimating CO_2 sources and sinks from atmospheric concentration measurements using a global inversion of atmospheric transport. Technical Reports – Max-Planck-Institut für Biogeochemie, 6, 53, 2005.

Schuster, U. and Watson, A. J.: A variable and decreasing sink for atmospheric CO_2 in the North Atlantic, J. Geophys. Res., 112, C11006, doi:10.1029/2006JC003941, 2007.

Sadourny, R. and Laval, K.: January and July performance of the LMD general circulation model, in: New Perspectives in Climate Modeling, edited by: Berger, A. L. and Nicolis, C., Elsevier Press, Amsterdam, 173–197, 1994.

Takahashi, T., Sutherland, S. C., and Kozyr, A.: Global Ocean Surface Water Partial Pressure of CO_2 Database: Measurements Performed During 1968–2008 (Version 2008). ORNL/CDIAC-152, NDP-088r. Carbon Dioxide Information Analysis Center, Oak Ridge National Laboratory, US Department of Energy, Oak Ridge, Tennessee, doi:10.3334/CDIAC/otg.ndp088r, 2009.

Tarantola, A.: Inverse Problem Theory and Methods for Model Parameter Estimation, Society for Industrial and Applied Mathematics, Philadephia, 2005.

Zimov, S. A., Schuur, E. A. G., and Chapin III, F. S.: Permafrost and the global carbon budget, Science, 312(5780), 1612–1613, doi:10.1126/science.1128908, 2006.

ACPD

10, 18561–18605, 2010

Table 1. Posterior uncertainties (in g C m^{-2} d^{-1}) and error reductions (in %) for weekly fluxes and posterior uncertainties (in g C m^{-2} yr^{-1}) for annual fluxes for one single region (France) and four selected groups of regions (Europe, Siberia, South America and North Atlantic (north of 30° N)) for all the OSSEs. The prior uncertainty is given in parenthesis.

	Weekly Fluxes (g C m^{-2} d^{-1} and %)										Annual Fluxes (g C m^{-2} yr^{-1})				
	France		Europe		Siberia		South America		North Atlantic		France	Europe	Siberia	South America	North North
	Post (2.63)	Err. Red	Post (0.6)	Err. Red	Post (0.6)	Err. Red	Post (1.51)	Err. Red	Post (0.04)	Err. Red	Post	Post	Post	Post	Post
EXISTSURF	0.35	86.9	0.22	63.2	0.25	53.0	0.86	43.7	0.03	34.1	19.47	19.46	19.88	75.27	2.85
HYPOSURF-A	0.53	80.1	0.05	92.1	0.04	91.2	0.04	97.2	0.02	51.2	30.46	2.53	1.80	2.45	1.57
HYPOSURF-B	0.61	76.8	0.05	91.9	0.05	88.7	0.12	92.1	0.02	48.6	36.68	2.62	2.62	7.29	1.77
A-SCOPE-2.0	0.51	80.6	0.06	89.4	0.05	87.0	0.08	94.9	0.02	45.5	29.70	3.51	2.55	3.23	1.93
A-SCOPE-1.6	0.51	80.6	0.05	89.8	0.05	86.6	0.05	96.4	0.02	48.0	29.96	3.43	2.60	2.46	1.80
OCO	0.73	72.1	0.10	81.3	0.09	74.3	0.10	93.6	0.03	34.3	47.15	6.50	6.06	4.18	2.72
GOSAT	1.06	59.7	0.15	71.5	0.15	60.3	0.25	83.4	0.04	12.6	80.77	10.79	11.05	10.65	4.49
SCIAMACHY	1.06	59.7	0.15	71.5	0.15	59.7	0.29	80.6	0.03	17.8	80.20	10.42	11.44	12.30	4.01
AIRS	2.12	19.7	0.28	49.3	0.33	31.3	0.23	84.6	0.04	4.8	261.48	24.03	34.06	11.39	5.28
HYPOSURF-A+ EXISTSURF	0.28	89.5	0.04	93.1	0.04	91.2	0.04	97.3	0.02	56.9	14.85	2.12	1.78	2.43	1.28
HYPOSURF-B+ EXISTSURF	0.29	89.0	0.04	93.1	0.05	89.1	0.12	92.1	0.02	54.1	15.61	2.19	2.46	7.24	1.49
A-SCOPE-2.0+ EXISTSURF	0.27	89.6	0.05	90.5	0.05	87.3	0.08	94.9	0.02	53.1	14.62	2.89	2.47	3.21	1.51
A-SCOPE-1.6+ EXISTSURF	0.27	89.6	0.05	90.9	0.05	87.0	0.05	96.4	0.02	55.2	14.61	2.84	2.51	2.45	1.41
OCO+EXISTSURF	0.31	88.3	0.08	85.3	0.08	77.3	0.10	93.6	0.02	46.7	16.58	4.71	4.93	4.14	1.92
GOSAT+EXISTSURF	0.33	87.5	0.11	80.5	0.13	68.5	0.25	83.6	0.02	38.2	18.12	6.48	7.77	10.27	2.53
SCIAMACHY+ EXISTSURF	0.33	87.5	0.11	79.6	0.13	68.0	0.29	80.8	0.02	39.5	18.08	6.79	8.0	11.91	2.42
AIRS+EXISTSURF	0.34	86.9	0.18	68.8	0.21	56.5	0.23	84.8	0.03	35.8	19.36	13.67	15.49	10.86	2.70
A-SCOPE-2.0+ AIRS+EXISTSURF	0.27	89.6	0.05	90.5	0.05	87.3	0.07	95.2	0.02	53.3	14.62	2.88	2.47	3.03	1.50
A-SCOPE-1.6+ AIRS+EXISTSURF	0.27	89.6	0.05	90.9	0.05	87.0	0.05	96.5	0.02	55.3	14.60	2.83	2.51	2.41	1.40
OCO+AIRS+ EXISTSURF	0.31	88.4	0.08	85.3	0.08	77.3	0.09	94.1	0.02	47.0	16.57	4.68	4.92	3.86	1.90
GOSAT+AIRS+ EXISTSURF	0.33	87.5	0.11	80.8	0.12	68.8	0.17	88.8	0.02	39.0	18.09	6.33	7.67	7.08	2.47

ACPD
10, 18561–18605, 2010

Table 2. Quantitative requirements for four different objectives discussed in this study.

Objective	Temporal scale	Spatial Scale (km)	Requirement
Vegetation dynamic	Weekly (target) Monthly (threshold)	200–1000	$0.3\,g\,C\,m^{-2}\,d^{-1}$
Land surface sources and sinks	Annual	2000	$5/25\,g\,C\,m^{-2}\,yr^{-1}$
Ocean sources and sinks	Annual	2500	$3\,g\,C\,m^{-2}\,yr^{-1}$
Anthropogenic Emissions	Annual	300	$4\,g\,C\,m^{-2}\,yr^{-1}$

ACPD
10, 18561–18605, 2010

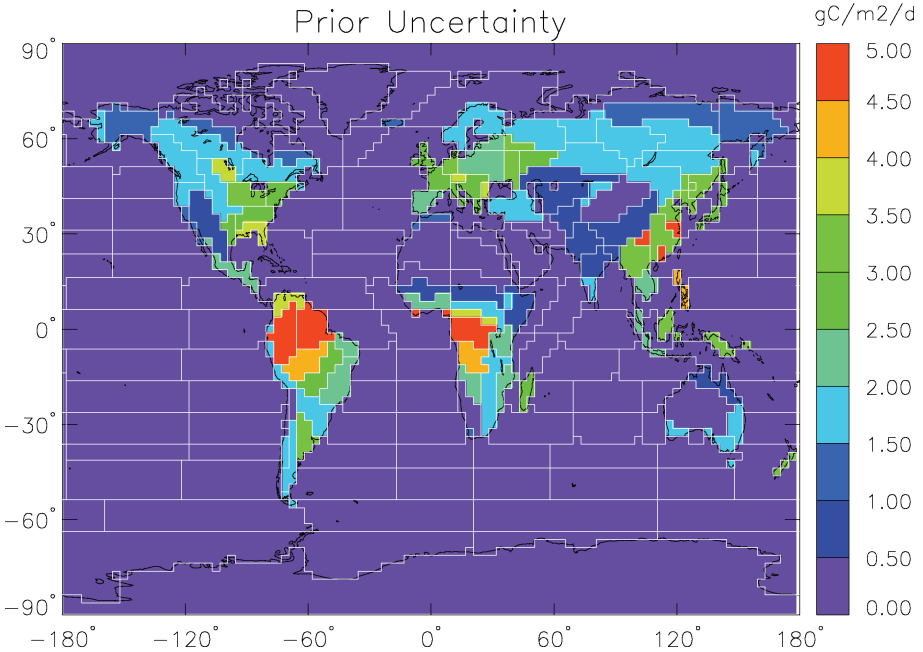

Fig. 1. Prior uncertainty of weekly fluxes in $g\,C\,m^{-2}\,d^{-1}$. The white lines show the borders of the 200 regions for which the surface fluxes are retrieved.

ACPD
10, 18561–18605, 2010

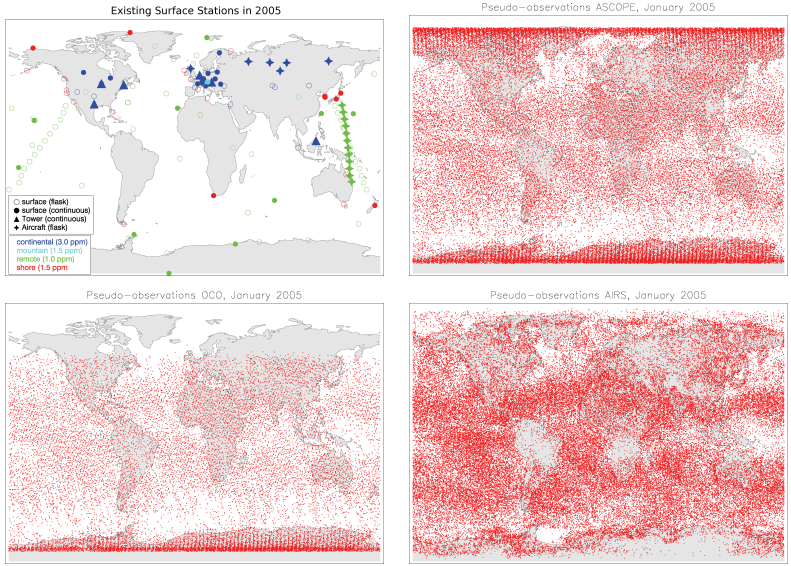

Fig. 2. (a) Geographical location of the existing surface stations in 2005. Different symbols are used to separate between the various measurement techniques, colours are indicative for the error associated with each station as mentioned in Sect. 3. Assumptions about the temporal sampling are described in Sect. 3. (b–d) clear-sky measurements of A-SCOPE-2.0 **(b)**, OCO **(c)** and AIRS **(d)** in January 2005.

ACPD
10, 18561–18605, 2010

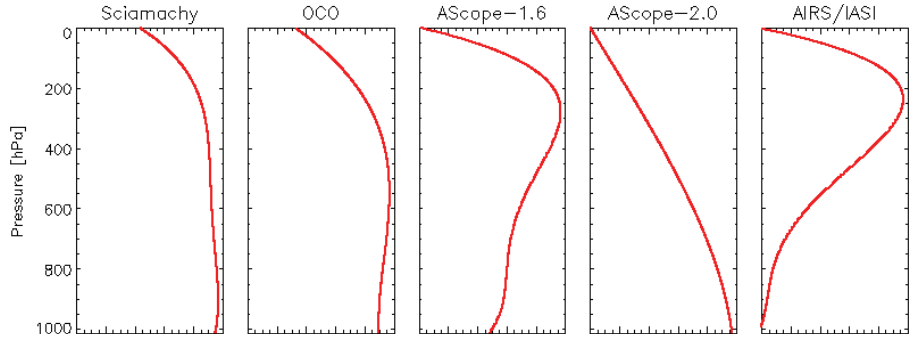

Fig. 3. Normalized vertical weighting functions for the satellite instruments considered in this study. The OCO weighting function is used for GOSAT too.

ACPD
10, 18561–18605, 2010

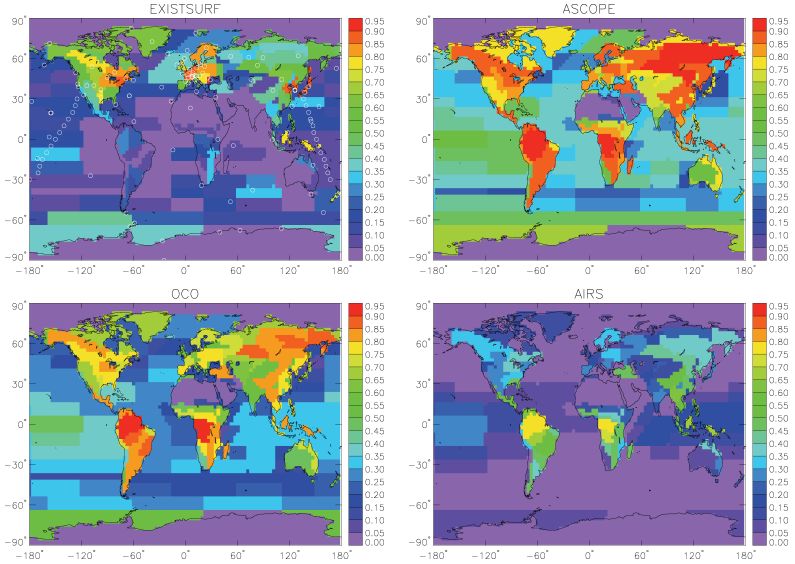

Fig. 4. Weekly mean error reduction for the **(a)** existing surface network (EXISTSURF) **(b)** A-SCOPE-2.0 **(c)** OCO **(d)** AIRS. White circles indicate the location of the surface stations.

ACPD
10, 18561–18605, 2010

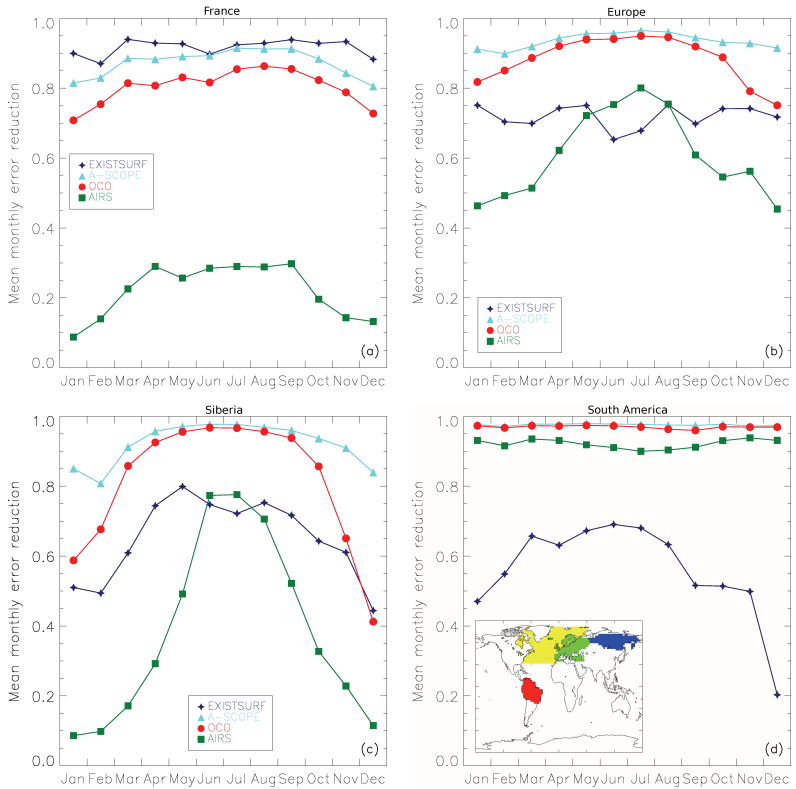

Fig. 5. Time series of the monthly error reduction of the monthly fluxes in **(a)** France, **(b)** Europe, **(c)** Siberia and **(d)** South America for four selected observing systems (EXISTSURF, A-SCOPE2.0, OCO and AIRS). The regions considered (aggregates of several of the pre-defined 200 regions) are also visualised in (d).

ACPD
10, 18561–18605, 2010

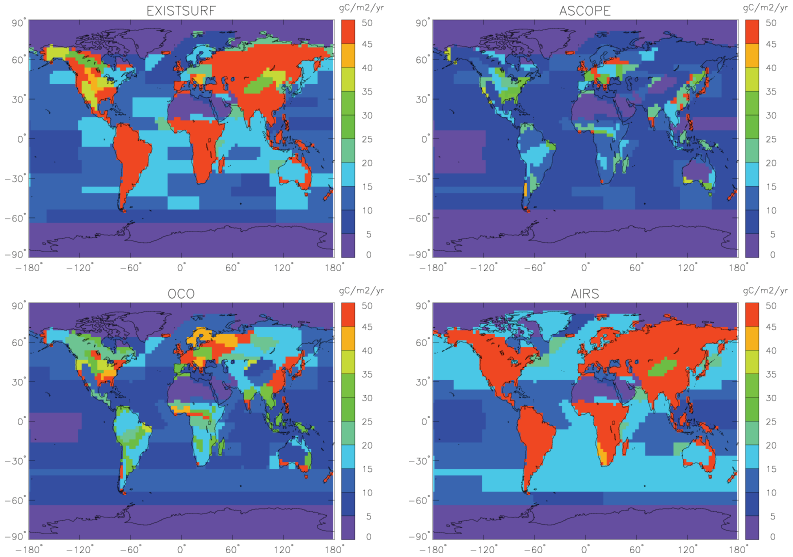

Fig. 6. Annual posterior uncertainty in g C m^{-2} yr^{-1} for the **(a)** existing surface network (EXISTSURF) **(b)** A-SCOPE-2.0 **(c)** OCO and **(d)** AIRS.

ACPD
10, 18561–18605, 2010